

5. Ellner, S. & Turchin, P. Chaos in a noisy world—new methods and evidence from time-series analysis. *Am. Nat.* **145**, 343–375 (1995).
6. Leirs, H. *et al.* Stochastic seasonality and nonlinear density-dependent factors regulate population size in an African rodent. *Nature* **389**, 176–180 (1997).
7. Moran, P. A. P. The statistical analysis of the Canadian lynx cycle: II synchronisation and meteorology. *Aust. J. Zool.* **1**, 291–298 (1953).
8. Ranta, E., Kaitala, V., Lindstrom, J. & Helle, E. The Moran effect and synchrony in population dynamics. *Oikos* **78**, 136–142 (1997).
9. Hill, J. K., Thomas, C. D. & Lewis, O. T. Effects of habitat patch size and isolation on dispersal by *Hesperia comma* butterflies: implications for metapopulation structure. *J. Anim. Ecol.* **65**, 725–735 (1996).
10. Bjornstad, O. N., Falck, W. & Stenseth, N. C. Geographic gradient in small rodent density fluctuations—a statistical modeling approach. *Proc. R. Soc. Lond. B* **262**, 127–133 (1995).
11. Jewell, P. A., Milner, C. & Morton-Boyd, J. *Island Survivors* (Athlone, London, 1974).
12. Clutton-Brock, T. H., Price, O. F., Albon, S. D. & Jewell, P. A. Persistent instability and population regulation in Soay sheep. *J. Anim. Ecol.* **60**, 593–608 (1991).
13. Grenfell, B. T., Price, O. F., Albon, S. D. & Clutton-Brock, T. H. Overcompensation and population cycles in an ungulate. *Nature* **355**, 823–826 (1992).
14. Sugihara, G. Red/blue chaotic power spectra. *Nature* **381**, 199–199 (1996).
15. Grenfell, B. T. Chance and chaos in measles dynamics. *J. R. Stat. Soc. B* **54**, 383–398 (1992).
16. Falck, W., Bjornstad, O. N. & Stenseth, N. C. Voles and lemmings—chaos and uncertainty in fluctuating populations. *Proc. R. Soc. Lond. B* **262**, 363–370 (1995).
17. Stenseth, N. C. Snowshoe hare populations—squeezed from below and above. *Science* **269**, 1061–1062 (1995).
18. Higgins, K., Hastings, A., Sarvela, J. N. & Botsford, L. W. Stochastic dynamics and deterministic skeletons: population behavior of Dungeness crab. *Science* **276**, 1431–1435 (1997).
19. Ranta, E., Kaitala, V., Lindstrom, J. & Linden, H. Synchrony in population dynamics. *Proc. R. Soc. Lond. B* **262**, 113–118 (1995).
20. Clutton-Brock, T. H. *et al.* Stability and instability in ungulate populations: an empirical analysis. *Am. Nat.* **149**, 195–219 (1997).
21. Hassell, M. P., Lawton, J. H. & May, R. M. Patterns of dynamical behaviour in single-species populations. *J. Anim. Ecol.* **45**, 471–486 (1976).
22. Turchin, P. Nonlinear time-series modeling of vole population fluctuations. *Res. Pop. Ecol.* **38**, 121–132 (1996).
23. Stenseth, N. C., Falck, W., Bjornstad, O. N. & Krebs, C. J. Population regulation in snowshoe hare and Canadian lynx: asymmetric food web configurations between hare and lynx. *Proc. Natl Acad. Sci. USA* **94**, 5147–5152 (1997).
24. Tong, H. *Non-linear Time Series: a Dynamical Systems Approach* (Oxford Univ. Press, 1990).
25. Tsay, R. S. Testing and modelling threshold autoregressive processes. *J. Am. Stat. Assoc.* **84**, 230–240 (1989).
26. Gulland, F. M. D. Role of nematode infections in mortality of Soay sheep during a population crash on St Kilda. *Parasitology* **105**, 493–503 (1992).
27. Grenfell, B. T., Wilson, K., Isham, V. S., Boyd, H. E. G. & Dietz, K. Modelling patterns of parasite aggregation in natural populations: trichostrongylid nematode-ruminant interactions as a case study. *Parasitology* **111**, S135–S151 (1995).
28. Framstad, E., Stenseth, N. C., Bjornstad, O. N. & Falck, W. Limit cycles in Norwegian lemmings: tensions between phase-dependence and density-dependence. *Proc. R. Soc. Lond. B* **264**, 31–38 (1997).
29. Cloete, S. W. P., Van Halderen, A. & Schneider, D. J. Causes of perinatal lamb mortality amongst dormer and SA mutton Merino lambs. *J. S. Afr. Vet. Assoc.* **64**, 121–125 (1993).
30. Champion, R. A., Rutter, S. M., Penning, P. D. & Rook, A. J. Temporal variation in grazing behavior of sheep and the reliability of sampling periods. *Appl. Anim. Behav. Sci.* **42**, 99–108 (1994).

Acknowledgements. We thank Scottish Natural Heritage and the National Trust for Scotland for permission to work on St Kilda, and their staff for assistance, support and encouragement; J. M. Pilkington, A. McColl, A. Robertson and I.R. Stevenson for help with the project; P. Rohani for comments on the manuscript; H. Tong for statistical advice and encouragement; and the Royal Artillery for logistical support on St Kilda. The work was funded by grants from the Natural Environment Research Council (to T.H.C.-B., M.J.C., B.T.G., K.W. and S.D.A.), the Royal Society (to M.J.C., K.W. and S.D.A.) and the Biotechnology and Biological Sciences Research Council (to J.M.P.).

Correspondence and requests for materials should be addressed to B.T.G. (e-mail: bryan@zoo.cam.ac.uk).

Cortical area MT and the perception of stereoscopic depth

Gregory C. DeAngelis*, Bruce G. Cumming† & William T. Newsome*

* Howard Hughes Medical Institute and Department of Neurobiology, Stanford University School of Medicine, Stanford, California 94305, USA
 † University Laboratory of Physiology, Parks Road, Oxford OX1 3PT, UK

Stereopsis is the perception of depth based on small positional differences between images formed on the two retinæ (known as binocular disparity). Neurons that respond selectively to binocular disparity were first described three decades ago^{1,2}, and have since been observed in many visual areas of the primate brain, including V1, V2, V3, MT and MST^{3–8}. Although disparity-selective neurons are thought to form the neural substrate for stereopsis, the mere existence of disparity-selective neurons does not

guarantee that they contribute to stereoscopic depth perception. Some disparity-selective neurons may play other roles, such as guiding vergence eye movements^{9,10}. Thus, the roles of different visual areas in stereopsis remain poorly defined. Here we show that visual area MT is important in stereoscopic vision: electrical stimulation of clusters of disparity-selective MT neurons can bias perceptual judgements of depth, and the bias is predictable from the disparity preference of neurons at the stimulation site. These

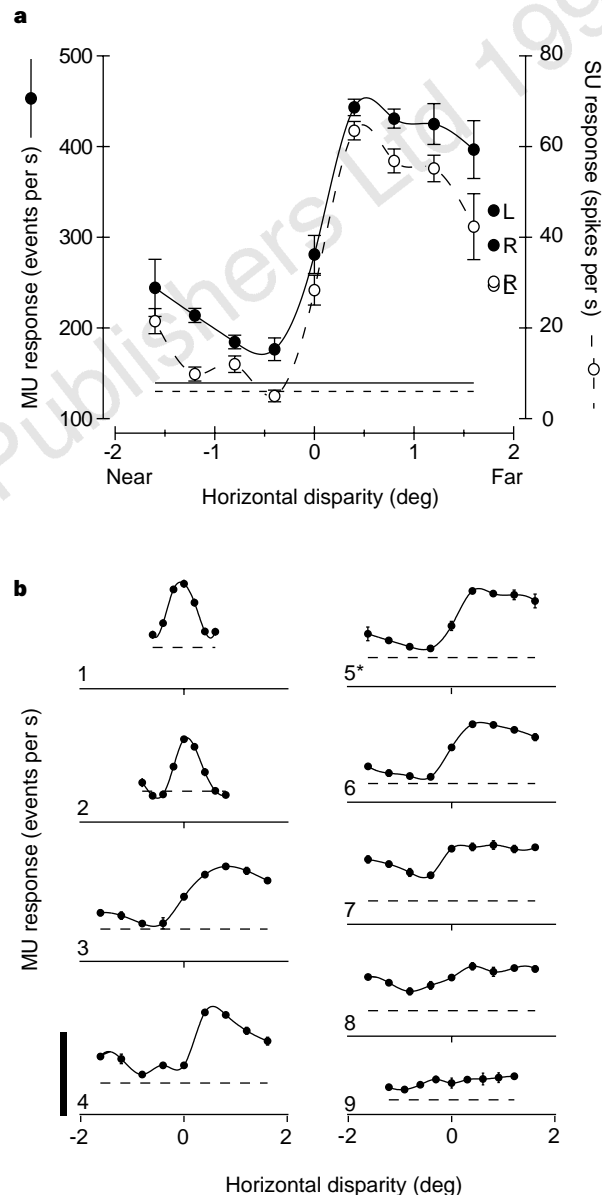


Figure 1 MT neurons are clustered according to disparity selectivity. **a**, Filled circles show multiunit (MU) responses to a drifting random-dot pattern; each datum is the mean of four responses ± 1 s.e. The solid curve is a cubic spline interpolation. Filled circles labelled 'L' and 'R' denote multiunit responses to the same visual stimulus presented monocularly to either the left or the right eye, respectively. The solid horizontal line gives the multiunit response in the absence of a visual stimulus (spontaneous activity). Open circles and the dashed curve show responses of an isolated single unit (SU) recorded simultaneously. The dashed horizontal line gives the spontaneous activity level of the single unit. **b**, Sequence of disparity-tuning curves recorded at 100 μ m intervals along an electrode penetration through MT in monkey S. Standard error bars are generally hidden by the data points. Curves are cubic spline interpolations, and dashed lines represent the spontaneous activity level. Height of scale bar is 400 events per second. Multiunit responses from site 5 (marked by an asterisk) are the same data shown in **a**.

results show that behaviourally relevant signals concerning stereoscopic depth are present in MT.

The middle temporal visual area (MT or V5) is important in motion perception¹¹. Most MT neurons are directionally selective, and these neurons are organized into a system of direction columns such that neurons in a particular column respond optimally to a specific direction of motion¹². Electrical microstimulation of a column of MT neurons can bias perceptual judgements of motion direction towards the direction encoded by the stimulated neurons^{13,14}. We have observed, however, that clusters of neighbouring MT neurons also respond optimally to a common range of preferred binocular disparities¹⁵. Figure 1a, for example, illustrates disparity tuning for a single unit and for a multiunit cluster, measured simultaneously from a single microelectrode. Action potentials from the single unit were excluded from the multiunit response, thus ensuring that the multiunit activity arose from several other nearby single units. The multiunit response is strongly tuned for disparity, indicating that its constituent single units have a similar disparity preference. This conclusion is further supported by the close agreement in shape between the multiunit and single-unit tuning curves; this correspondence is typical of most of our recordings in MT. Roughly half of the multiunit recording sites in MT showed strong disparity tuning (disparity-tuning index > 0.5; see Methods). When multiunit clusters were unselective for disparity, simultaneously recorded single units were generally unselective as well, eliminating the possibility that weak multiunit tuning results from combinations of single units tuned to widely different disparities.

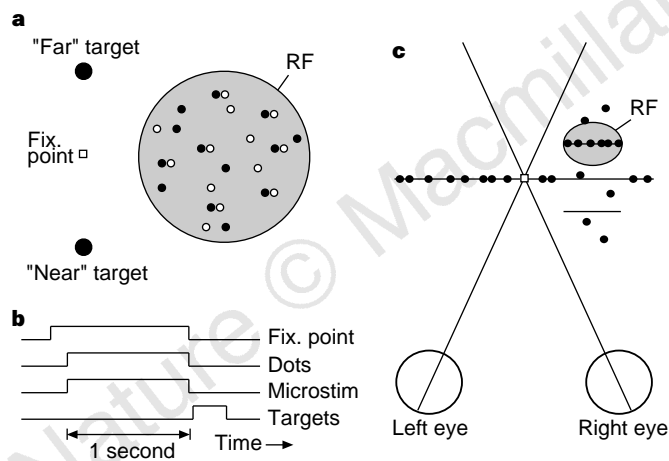


Figure 2 Depth-discrimination task. **a**, Spatial arrangement of fixation point, visual stimulus and response targets. A random-dot pattern was presented within a circular aperture that was roughly the same size as the multiunit receptive field (RF; shaded circle). Filled dots denote the image shown to the left eye, and unfilled dots indicate the image shown to the right eye. Half of the dots are shown paired with a fixed disparity ('signal' dots), and the remaining dots have random horizontal disparities ('noise' dots). **b**, Sequence of trial events. The fixation point appeared first, and the monkey was required to maintain fixation within a $\pm 1.5^\circ$ window throughout the trial. After fixation, the random-dot pattern appeared for 1 second. In half the trials, selected randomly, microstimulation was applied concurrently with the dots. Subsequently, fixation point, visual stimulus and microstimulation were turned off, and two small target disks appeared. The monkey made a saccadic eye movement to the upper target to indicate a far stimulus, or to the lower target to indicate a near stimulus. **c**, Top-down view of the visual stimulus. In each trial, signal dots appeared at one of two fixed disparities, one near and one far (short horizontal line segments). One disparity (far in this example) was chosen to be optimal for the recorded neurons; the other disparity was chosen to be non-optimal. Here, the visual stimulus consists of 50% signal dots and 50% noise dots. Signal and noise dots moved with a velocity (direction and speed) that was optimal for the neurons at the electrode tip. Dots situated along the plane of fixation (long horizontal line) were stationary and provided a zero-disparity background.

Figure 1b shows a sequence of disparity-tuning curves measured at 100- μm intervals along an oblique electrode penetration through MT. At recording sites 1 and 2, the multiunit activity was well tuned, with a preference for zero disparity. At site 3, there was a transition to broader tuning with a strong preference for far (positive) disparities over near disparities. This pattern was maintained over a span of about 300 μm (sites 3–6), after which the disparity tuning gradually became weaker, from site 7 to site 9. In other penetrations, regions of poor disparity tuning could span 1 mm or more, and were usually followed by regions of strong tuning. Thus, strongly disparity-tuned neurons are found within discrete patches in MT. The presence of extended regions of similar disparity tuning, such as sites 3–6 in Fig. 1b, is reminiscent of the well-known clustering of MT neurons by preferred direction, which we have exploited in previous microstimulation studies¹³. We therefore tested the role of MT in depth perception by applying electrical stimulation to disparity-tuned sites while two monkeys performed a stereoscopic depth-discrimination task. To activate a cluster of MT neurons with similar tuning, we applied stimulation to sites in which multiunit disparity tuning remained fairly constant over at least 200–300 μm (for example, sites 3–6 in Fig. 1b).

Figure 2 illustrates the depth-discrimination task. Monkeys viewed a random-dot visual display in which a fraction of the dots carried a consistent depth signal ('signal' dots), whereas the remaining dots were randomly scattered in depth ('noise' dots). In each trial, signal dots were presented at either a near or a far disparity, one of which was chosen to be optimal for the MT neurons recorded at the electrode tip. We chose other parameters of the visual stimulus (location, size, direction and speed of motion) to maximize the multiunit response. The monkey's task was to report seeing near or far depth by making a saccadic eye movement to one of two small visual targets. We varied task difficulty by adjusting the fraction of signal dots in the visual display (per cent binocular correlation). If microstimulation augments the signal carried by the stimulated neurons, and if these neurons provide signals used by the monkey in performing the task, then microstimulation should bias the monkey's choices in favour of the preferred disparity at the stimulation site. Importantly, the monkey was always rewarded for correctly reporting the actual depth of the signal dots, irrespective of the presence or absence of microstimulation. Thus the reward contingencies always encouraged veridical performance.

Figure 3 shows the results from two experiments in which microstimulation produced a bias toward the preferred disparity. Figure 3a depicts the multiunit disparity-tuning curve for a stimulation site that preferred far disparities, and the effect of microstimulation at this site on the monkey's psychophysical judgements is shown in Fig. 3b. At almost every binocular correlation level, the monkey made more 'preferred' decisions in stimulated trials than in non-stimulated trials. The net effect of this preferred disparity bias is a leftward shift of the psychometric function, which we measured as the horizontal offset between sigmoidal curves that were fitted to the data using logistic regression. In this experiment, the shift was equivalent to 22.5% correlated dots, an average-sized effect for monkey R.

Figure 3c shows the disparity-tuning curve for a stimulation site in monkey T that preferred near disparities. Again, microstimulation biased the animal's choices toward the preferred (near) disparity of the stimulated neurons. The leftward shift of the psychometric function was equivalent to 57.6% correlated dots (Fig. 3d), the largest effect that we have observed so far.

Figure 4 summarizes results from 65 microstimulation experiments performed in two monkeys. The scatter plot shows the size of the microstimulation effect plotted against the disparity-tuning index (DTI) of multiunit activity at each stimulation site. Positive values on the ordinate correspond to leftward shifts of the psychometric function, that is, shifts toward the preferred disparity of the stimulated neurons. Filled symbols indicate statistically significant

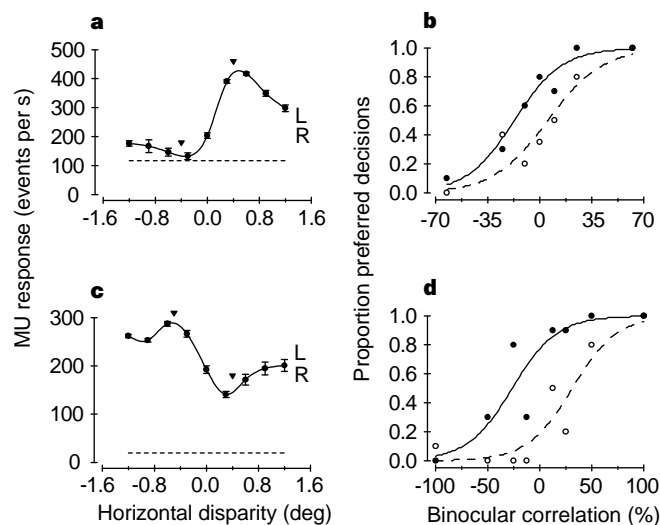


Figure 3 Microstimulation of MT biases depth judgements. **a**, Disparity tuning of multiunit activity at a site in monkey R that prefers far disparities. Arrowheads denote the two disparities used in the discrimination task. L and R denote multiunit responses to the same visual stimulus presented monocularly to either the left or the right eye, respectively. **b**, Effect of microstimulation on depth judgements for the site depicted in **a**. The abscissa gives the percentage of binocularly correlated dots (that is, the percentage of 'signal' dots). Positive values indicate that signal dots were presented at the preferred disparity; negative values correspond to signal dots presented at the non-optimal disparity. The ordinate shows the proportion of decisions made in favour of the preferred disparity (10 trials per point). Filled and open circles correspond to trials with and without microstimulation, respectively. The effect of microstimulation was highly significant (logistic regression, $P < 0.005$). **c**, Disparity tuning of multiunit activity at a near-tuned site in monkey T. **d**, Effect of microstimulation at the site for which tuning is shown in **c**. This effect was also significant ($P < 0.0001$).

effects (logistic regression¹⁶, $P < 0.05$), which occurred in 43 of 65 experiments. Among the significant effects, 42 of 43 were in the direction predicted by the disparity tuning of the multiunit activity; the one exception occurred at a site with weak disparity tuning. In contrast, microstimulation had a significant effect on the slope of the psychometric function in only 4 of 65 experiments. The mean slope ratio (stimulation versus no stimulation) was 0.97, which is not significantly different from 1.0 (t -test, $t = -0.68$, $P > 0.5$, $N = 65$).

The strength of the microstimulation effect was significantly correlated with the DTI of the stimulated neurons ($R = 0.44$, $P < 0.001$), with no significant difference between the two monkeys (analysis of covariance, $P = 0.08$). Statistically significant microstimulation effects were generally limited to sites with moderate to strong disparity selectivity. This correlation is reassuring because it provides an additional internal control for nonspecific effects of microstimulation: the effects at weakly tuned sites should be small, and they are.

In the experiments described above, dots always moved in the preferred direction of the stimulated MT neurons. We also tested whether the effects of microstimulation on depth judgements were limited to moving stimuli. We trained monkey R to perform the depth-discrimination task (Fig. 2) when all dots were stationary. Thus, the only image motion on the retina would be that induced by small eye movements made during fixation. We used stationary dots to study 12 MT sites at which microstimulation produced a significant effect when moving dots were used. For 9 of these 12 sites, microstimulation also produced a significant preferred bias when using stationary dots; at the remaining 3 sites there was no significant effect. The mean leftward shift of the psychometric function across all 12 sites was 25.8% for moving dots and 27.9%

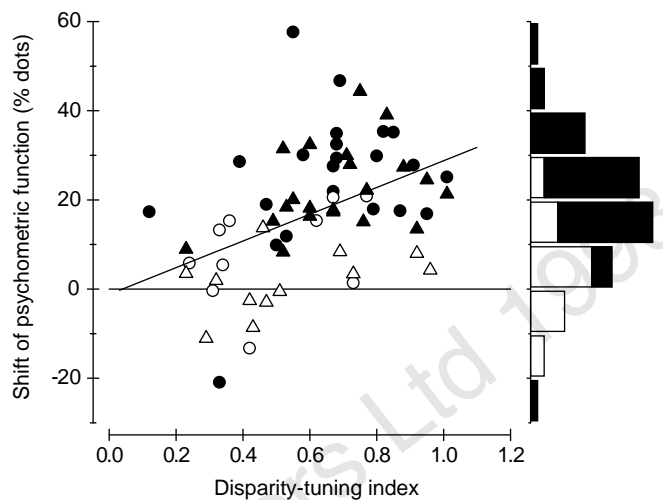


Figure 4 Summary of microstimulation effects from 65 experiments using two monkeys. The scatter plot shows the shift of the psychometric function plotted against the disparity-tuning index of multiunit activity measured at each stimulation site. Filled symbols denote significant effects (logistic regression, $P < 0.05$). Triangles and circles indicate data from monkeys R and T, respectively. The solid line shows the best linear fit to the data (linear regression). On the right, the data are collapsed across the disparity-tuning index and plotted as a histogram.

for stationary dots ($P > 0.5$; paired t -test). We also measured disparity-tuning curves at these 12 sites using stationary dots. All sites exhibited strong disparity selectivity for stationary dots (mean DTI, 0.93 for stationary and 0.70 for moving dots; $P < 0.001$, paired t -test), although the peak response rate was generally smaller for stationary dots (223 events per second) than for moving dots (371 events per second) ($P < 0.001$, paired t -test). Some of the response to stationary dots seemed to be driven by small eye movements during fixation. As these occur under natural viewing conditions, MT neurons may normally be active during viewing of stationary objects.

Our results show that the disparity signals carried by MT neurons are an important part of the neural substrate for depth judgements in our task. This finding establishes the first direct link between the neural property of disparity selectivity and the perceptual capacity for stereopsis, and complements the results of recent studies using both psychophysics and physiology that found a role for MT in the perception of depth from motion cues^{17,18}. Our results also show that the role of MT in vision is not limited to analysis of moving objects, because many MT neurons exhibit robust disparity tuning in response to stationary random-dot patterns, and microstimulation biases depth judgements of stationary dots. Although MT is important in stereopsis under the conditions of our experiment, this does not mean that all aspects of stereopsis depend on MT, nor that any single aspect of stereopsis depends entirely on MT. In this respect, it is interesting to note that a previous study, using a substantially different stereo task, found no effect of MT lesions on psychophysical performance¹⁹. Broadly based investigations, combining a variety of perceptual tests with multiple physiological probes of neural function, will be necessary to achieve a comprehensive understanding of the neural basis of stereoscopic vision. □

Methods

Our methods for physiological recording and microstimulation in awake monkeys have been described previously^{13,20}. We used three rhesus monkeys, two males and one female. During experimental sessions, the monkey was seated in a primate chair with its head restrained, and eye position was monitored using the scleral search coil technique^{21,22}. Two monkeys (R and S) had eye coils implanted in both eyes, to allow monitoring of vergence eye

movements. Systematic changes in vergence angle were not observed as a result of any of the experimental manipulations described below. Tungsten micro-electrodes (impedance typically 250–750 k Ω at 1 kHz) were inserted into the cortex through a transdural guide tube, and event times were stored with 1-ms resolution. Any deflection of the neural signal that exceeded a threshold level was classified as a multiunit event using a bilevel window discriminator. Thus, an increase in amplitude of the neural 'hash' was registered as an increase in frequency of the multiunit activity, which we express in events per second. The absolute frequency of the multiunit response depended on the level of the event threshold and the frequency passband of the amplifier (which was fixed). We attempted to adjust the threshold level to maintain a roughly constant frequency of spontaneous activity from site to site within a penetration. In some experiments (for example, that shown in Fig. 1a), well-isolated action potentials were simultaneously recorded as single units using a template-based spike discriminator. These spikes were excluded from the multiunit response by setting the upper level of the window discriminator below the peak of the spikes. In general, we found the multiunit response to be an excellent predictor of the disparity tuning of single units that were recorded simultaneously at 43 sites in monkey S. Tuning curves constructed from multiunit responses also agreed closely with those computed from the root-mean-square amplitude of the local field potential (bandpass filtered from 20–200 Hz). Monkeys received a liquid reward for correct completion of each trial. Animal care and all experimental procedures conformed to guidelines established by the National Institutes of Health.

Disparity-tuning measurements. The monkey was simply required to maintain fixation on a small spot while a moving random-dot pattern appeared over the multiunit receptive field. Location, size and movement speed of the random-dot pattern were tailored to the preference of the neurons at each recording site. The dots were rendered in depth as red/green anaglyphs viewed at a distance of 57 cm through red and green filters (Kodak Wratten numbers 29 and 61, respectively). Outside the receptive field, the remainder of the visual display (which subtended 30° × 23°) was filled with zero-disparity dots, which were replotted randomly at 20 Hz to produce a flickering background. The zero-disparity background helped to maintain the monkey's vergence at the depth of the fixation point. The video display was refreshed at 60 Hz.

In the experiment shown in Fig. 1b, disparity tuning was measured along an oblique penetration through MT. We approached MT from the occipital lobe; electrodes travelled caudal to rostral in a sagittal plane. The electrode trajectory was tilted 20° away from horizontal. Thus, our electrode passed through MT at an oblique angle, ranging from ~45–90° away from the normal. We recorded multiunit activity at regularly spaced intervals of 100 μ m. When possible, we also isolated spikes from a single unit and recorded these on a separate channel (Fig. 1a).

Disparity-tuning curves were fitted with a cubic spline interpolation. The DTI was defined as: $1 - (R_{\min} - S)/(R_{\max} - S)$, where R_{\max} is the maximum fitted response, R_{\min} is the minimum fitted response, and S denotes spontaneous activity (in the absence of a visual stimulus). Large values of DTI (near 1.0) correspond to strong disparity tuning, and values near zero correspond to weak tuning. For sites with significant disparity tuning (one-way analysis of variance $P < 0.05$), the disparity at which the fitted curve reached a maximum defined the preferred disparity.

Microstimulation experiments. We trained two monkeys (R and T) to perform the depth-discrimination task shown in Fig. 2. To identify candidate microstimulation sites, we searched for regions of MT where the disparity tuning of multiunit activity was roughly constant over at least 200–300 μ m (for example, sites 3–6 in Fig. 1b), and we positioned our electrode in the middle of that region. Microstimulation parameters were similar to those used in previous studies of motion discrimination^{13,23}. The stimulation train consisted of 20- μ A biphasic pulses, each consisting of a 200- μ s cathodal pulse followed by a 200- μ s anodal pulse, with a 100- μ s interval in between. Visual stimuli were presented stereoscopically by alternating left and right half-images at 100 Hz while the monkey viewed the display through ferro-electric shutter glasses that were synchronized to the video refresh. The random-dot stimulus was displayed using the red gun on a standard RGB display, because the red phosphor has the fastest decay time and allows the best stereo separation.

Received 13 April; accepted 1 June 1998.

- Barlow, H. B., Blakemore, C. & Pettigrew, J. D. The neural mechanism of binocular depth discrimination. *J. Physiol. (Lond.)* **193**, 327–342 (1967).
- Pettigrew, J. D., Nikara, T. & Bishop, P. O. Binocular interaction on single units in cat striate cortex: simultaneous stimulation by single moving slit with receptive fields in correspondence. *Exp. Brain Res.* **6**, 391–410 (1968).
- Hubel, D. H. & Wiesel, T. N. Stereoscopic vision in macaque monkey. Cells sensitive to binocular depth in area 18 of the macaque monkey cortex. *Nature* **225**, 41–42 (1970).
- Poggio, G. F. & Fischer, B. Binocular interaction and depth sensitivity in striate and prestriate cortex of behaving rhesus monkey. *J. Neurophysiol.* **40**, 1392–1405 (1977).
- Poggio, G. F., Gonzalez, F. & Krause, F. Stereoscopic mechanisms in monkey visual cortex: binocular correlation and disparity selectivity. *J. Neurosci.* **8**, 4531–4550 (1988).
- Felleman, D. J. & Van Essen, D. C. Receptive field properties of neurons in area V3 of macaque monkey extrastriate cortex. *J. Neurophysiol.* **57**, 889–920 (1987).
- Maunsell, J. H. & Van Essen, D. C. Functional properties of neurons in middle temporal visual area of the macaque monkey. II. Binocular interactions and sensitivity to binocular disparity. *J. Neurophysiol.* **49**, 1148–1167 (1983).
- Roy, J. P., Komatsu, H. & Wurtz, R. H. Disparity sensitivity of neurons in monkey extrastriate area MST. *J. Neurosci.* **12**, 2478–2492 (1992).
- Cumming, B. G. & Parker, A. J. Responses of primary visual cortical neurons to binocular disparity without depth perception. *Nature* **389**, 280–283 (1997).
- Masson, G. S., Busetini, C. & Miles, F. A. Vergence eye movements in response to binocular disparity without depth perception. *Nature* **389**, 283–286 (1997).
- Albright, T. D. Cortical processing of visual motion. *Rev. Oculomotor Res.* **5**, 177–201 (1993).
- Albright, T. D., Desimone, R. & Gross, C. G. Columnar organization of directionally selective cells in visual area MT of the macaque. *J. Neurophysiol.* **51**, 16–31 (1984).
- Salzman, C. D., Murasugi, C. M., Britten, K. H. & Newsome, W. T. Microstimulation in visual area MT: effects on direction discrimination performance. *J. Neurosci.* **12**, 2331–2355 (1992).
- Salzman, C. D. & Newsome, W. T. Neural mechanisms for forming a perceptual decision. *Science* **264**, 231–237 (1994).
- DeAngelis, G. C., Groh, J. M. & Newsome, W. T. Organization of disparity selectivity in macaque area MT. *Soc. Neurosci. Abstr.* **22**, 717 (1996).
- Cox, D. R. & Snell, E. J. *Analysis of Binary Data* (Chapman and Hall, London, 1989).
- Bradley, D. C., Chang, G. C. & Andersen, R. A. Encoding of three-dimensional structure-from-motion by primate area MT neurons. *Nature* **392**, 714–717 (1998).
- Dodd, J. V., Cumming, B. G., Newsome, W. T. & Parker, A. J. Firing of V5 (MT) neurons reliably covaries with reported 3-D configuration in a perceptually-ambiguous structure-from-motion task. *Soc. Neurosci. Abstr.* **23**, 1125 (1997).
- Schiller, P. H. The effects of V4 and middle temporal (MT) area lesions on visual performance in the rhesus monkey. *Vis. Neurosci.* **10**, 717–746 (1993).
- Britten, K. H., Shadlen, M. N., Newsome, W. T. & Movshon, J. A. The analysis of visual motion: a comparison of neuronal and psychophysical performance. *J. Neurosci.* **12**, 4745–4765 (1992).
- Robinson, D. A. A method of measuring eye movement using a scleral search coil in a magnetic field. *IEEE Trans. Biomed. Eng.* **10**, 137–145 (1963).
- Judge, S. J., Richmond, B. J. & Chu, F. C. Implantation of magnetic search coils for measurement of eye position: an improved method. *Vision Res.* **20**, 535–538 (1980).
- Murasugi, C. M., Salzman, C. D. & Newsome, W. T. Microstimulation in visual area MT: effects of varying pulse amplitude and frequency. *J. Neurosci.* **13**, 1719–1729 (1993).

Acknowledgements. We thank J. Stein and C. Doane for technical assistance, and A. Parker, J. Dodd, B. Wandell, J. Nichols, E. Siedemann, G. Horwitz, and C. Barberini for critical review of the manuscript. G.C.D. was supported by a Medical Research Fellowship from the Bank of America/Giannini Foundation, an NRSA from the National Eye Institute, and a Career Award in the Biomedical Sciences from the Burroughs-Wellcome Fund. B.G.C. is a Royal Society Research Fellow, and W.T.N. is an Investigator of the Howard Hughes Medical Institute. This work was also supported by the National Eye Institute.

Correspondence and requests for materials should be addressed to W.T.N. (e-mail: bill@monkeybiz.stanford.edu).

Maintenance of late-phase LTP is accompanied by PKA-dependent increase in AMPA receptor synthesis

Asha Nayak*†, Devon J. Zastrow*†, Ronald Lickteig‡, Nancy R. Zahniser†‡ & Michael D. Browning†‡

‡ Department of Pharmacology and † Neuroscience Program, University of Colorado Health Sciences Center, 4200 East Ninth Avenue, Denver, Colorado 80262, USA

* These authors contributed equally to this work

Long-term potentiation (LTP) is a form of synaptic plasticity that has been extensively studied as a putative mechanism underlying learning and memory. A late phase of LTP occurring 3–5 hours after stimulation and depending on transcription, protein synthesis and cyclic-AMP-dependent protein kinase (protein kinase A, or PKA) has been described^{1–3}, but it is not known whether transcription of presynaptic and/or postsynaptic genes is required to support late-phase LTP. Here we show that late-phase LTP can be obtained in rat hippocampal CA1 mini-slices